Cancer Research

CD38-Driven Mitochondrial Trafficking Promotes Bioenergetic Plasticity in Multiple Myeloma

Christopher R. Marlein[1], Rachel E. Piddock[1], Jayna J. Mistry[1], Lyubov Zaitseva[1], Charlotte Hellmich[1,2], Rebecca H. Horton[1], Zhigang Zhou[1], Martin J. Auger[2], Kristian M. Bowles[1,2], and Stuart A. Rushworth[1]

Abstract

Metabolic adjustments are necessary for the initiation, proliferation, and spread of cancer cells. Although mitochondria have been shown to move to cancer cells from their microenvironment, the metabolic consequences of this phenomenon have yet to be fully elucidated. Here, we report that multiple myeloma cells use mitochondrial-based metabolism as well as glycolysis when located within the bone marrow microenvironment. The reliance of multiple myeloma cells on oxidative phosphorylation was caused by intercellular mitochondrial transfer to multiple myeloma cells from neighboring nonmalignant bone marrow stromal cells. This mitochondrial transfer occurred through tumor-derived tunneling nanotubes (TNT). Moreover, shRNA-mediated knockdown of CD38 inhibits mitochondrial transfer and TNT formation *in vitro* and blocks mitochondrial transfer and improves animal survival *in vivo*. This study describes a potential treatment strategy to inhibit mitochondrial transfer for clinical benefit and scientifically expands the understanding of the functional effects of mitochondrial transfer on tumor metabolism.

Significance: Multiple myeloma relies on both oxidative phosphorylation and glycolysis following acquisition of mitochondria from its bone marrow microenvironment.

See related commentary by Boise and Shanmugam, p. 2102

Introduction

The process by which a rapidly proliferating cancer cell fuels its metabolic requirements is a highly attractive therapeutic target. Warburg stated in 1956 that malignant cells generally use the nonmitochondrial-based method of glycolysis to generate its ATP requirements (1). Multiple myeloma is a hematologic malignancy characterized by the accumulation of monoclonal plasma cells within the bone marrow (2) and is reported to be reliant on glycolysis due to its susceptibility to glycolysis inhibitors such as dichloroacetate (3), as well as an elevated glycolytic gene profile (4). However, multiple myeloma cells do have the capability of using mitochondrial-based oxidative phosphorylation under ritonavir treatment (5) and HIF-1α suppression (6).

Oxidative phosphorylation generates a larger quantity of ATP than glycolysis and occurs within the mitochondria of eukaryotic cells (7). This organelle was originally thought to reside in its somatic cell for its life; however, the Gerdes laboratory showed that mitochondria can move between cells (8). This phenomenon has now been reported in models of human cancer including lung (9), bladder (10), breast (11), and melanoma (12, 13). Mitochondrial transfer has also recently been shown pathophysiologically, not using models, in canine transmissible cancer (14). Bone marrow stromal cells (BMSC), which reside in the multiple myeloma microenvironment, have been shown to be donors in malignant mitochondrial transfer to acute myeloid leukemia blasts (15, 16) and nonmalignant transfer to lung epithelial cells (17). Others have shown nonmalignant transfer of mitochondrial from astrocytes to neurons after stroke is controlled by CD38 (18). These studies indicate that the trafficking of mitochondrial between cells has a role in adapting metabolic processes in both nonmalignant and malignant cells.

Multiple myeloma is currently incurable with only half of patients surviving beyond 5 years after diagnosis (19). Multiple myeloma is a tumor highly dependent on the bone marrow microenvironment (BMM), which functions in a supportive role to promote tumor proliferation, survival, and migration (20). Preclinical studies of CD38 inhibition in myeloma show that it mediates multiple myeloma cytotoxicity in the presence of the protective bone marrow niche (21), and in early-phase clinical studies, anti-CD38–directed therapy showed clinical benefit as a single agent in myeloma patients (22, 23). Furthermore, phase III clinical trials in multiple myeloma patients of anti-CD38 antibody therapy given in addition to chemotherapy have demonstrated improvements in overall response rates and progression-free survival (24, 25) and lower risk of death (26) in patients receiving the antibody with chemotherapy compared with chemotherapy alone. Daratumumab has now been FDA approved for the treatment of relapse-refractory myeloma in combination with bortezomib or lenalidomide (27).

In this study, we look to determine first if the multiple myeloma microenvironment supports multiple myeloma proliferation, by

[1]Norwich Medical School, The University of East Anglia, Norwich Research Park, Norwich, United Kingdom. [2]Department of Haematology, Norfolk and Norwich University Hospitals NHS Trust, Norwich, United Kingdom.

Note: Supplementary data for this article are available at Cancer Research Online (http://cancerres.aacrjournals.org/).

Corresponding Authors: Stuart A. Rushworth, University of East Anglia, Norwich Research Park, Norwich, Norfolk NR4 7TJ, United Kingdom. Phone: 075-472-54801; Fax: 016-035-93752; E-mail: s.rushworth@uea.ac.uk; and Kristian M. Bowles, k.bowles@uea.ac.uk

doi: 10.1158/0008-5472.CAN-18-0773

promoting mitochondrial-based oxidative phosphorylation. Second, we analyze whether the transfer of mitochondria to malignant plasma cells, from BMSC, regulates the metabolic process. Next, we aim to dissect the mechanisms that facilitate the interaction allowing the BMSC to transfer mitochondria to multiple myeloma. Finally, we aim provide a novel therapeutic paradigm for the targeting of mitochondrial transfer as an anticancer therapy.

Materials and Methods

Primary cell culture

Patient bone marrow was obtained following informed written consent and under approval by the Health Research Authority of the National Health Service, United Kingdom (LRECref07/H0310/146) and in accordance with the Declaration of Helsinki. All patient details are provided in Table 1. Primary multiple myeloma cells were isolated by histopaque density centrifugation and purified by positive selection using magnetic-activated cell sorting with $CD138^+$ microbeads (Miltenyi Biotec), and cell type was confirmed by flow cytometry as previously described (28). BMSCs were isolated from multiple myeloma patient samples by adherence to tissue culture plastic and were then expanded in DMEM containing 10% FBS and supplemented with 1% penicillin–streptomycin (Hyclone; Life Sciences; ref. 29). BMSC markers were confirmed using flow cytometry for expression of $CD90^+$, $CD73^+$, $CD105^+$, and $CD45^-$. BMSCs were passaged 3 times before use in the assays presented in this article (30).

Human cell lines

The multiple myeloma–derived cell lines were obtained from the European Collection of Cell Cultures where they are authenticated by DNA fingerprinting. The cells were periodically tested for *Mycoplasma* contamination, using the MycoProbe, Mycoplasma Detection Kit purchased from R&D Systems in January 2018. These cells were cultured in Roswell Park Memorial Institute (RPMI) 1640 medium supplemented with 10% FBS and 1% penicillin–streptomycin (Hyclone, Life Sciences). All cell lines were used between passages 4 and 15 from the time of purchase.

MitoTracker-based mitochondrial transfer assay

To assess and quantify mitochondrial transfer from BMSC to multiple myeloma cells, the MitoTracker-based staining assay developed in our laboratory was used (15). Briefly, human primary BMSCs were stained with 200 nmol/L MitoTracker Green FM for 1 hour. Primary and cell line multiple myeloma were also stained with 200 nmol/L MitoTracker Green FM for 30 minutes, to eliminate dye leakage. Both cell types were washed 3 times in PBS to remove the unbound probe. Stained multiple myeloma cells were added to stained BMSC at a 5:1 ratio for 24 hours. Stained multiple myeloma cells were also grown in monoculture for 24 hours as a control. After incubation, multiple myeloma cells were removed from BMSC, and MitoTracker fluorescence in these cells was analyzed using the CyFlow Cube 6 flow cytometer (Sysmex, Milton Keynes). For mitochondrial quantification, the difference in MitoTracker fluorescence between multiple myeloma cells grown with and without BMSC provided a baseline mitochondrial transfer. The effect of cytochalasin B (350 μmol/L), Dansylcadavarine (50 μmol/L), bortezomib (10 nmol/L), CD38-blocking antibody, or CD38 knockdown (KD) multiple myeloma cells on mitochondrial transfer was achieved using this method.

Table 1. Patient information of primary multiple myeloma samples used in this study

Multiple myeloma#	Sex	Age	Isotype	% Plasmacytosis
#1	M	82	IgG	90
#2	F	76	Kappa LC	70
#3	F	79	IgA	90
#4	F	75	Lambda LC	65
#5	M	90	IgG	90
#6	M	96	IgG	25
#7	F	89	IgG	30
#8	M	62	IgG	65
#9	F	75	IgA	50
#10	M	73	Kappa LC	75
#11	M	78	IgG	90

rLV.EF1.mCherry mitochondrial transfer assay

rLV.EF1.mCherry lentivirus was purchased from Clontech Takara Bio Europe. Primary human BMSCs were transduced with this virus for 72 hours and cultured for 1 week before use, to ensure no residual lentivirus remained. RPMI cells were cultured with rLV.EF1.mCherry BMSC for 1 week and imaged using the Zeiss LSM 800 Axio Observer.Z1 confocal microscope with a 40X water objective (Carl Zeiss).

Multiple myeloma xenograft model

For this study, the NOD.Cg-Prkdcscid IL2rgtm1Wjl/SzJ (NSG) mice (The Jackson Laboratory; RRID:IMSR_NM-NSG-001) were housed under specific pathogen-free conditions in a 12/12-hour light/dark cycle with food and water provided *ad libitum* in accordance with the Animal Scientific Procedures Act, 1986 (UK), and under UK Home Office and Institutional Animal Welfare and Ethics Review board approvals. Note that 0.5×10^6 MM1S or U266 multiple myeloma cell lines were i.v. injected into nonirradiated 6- to 8-week-old NSG mice for mouse mtDNA detection. MM1S-luc cells (1.0×10^6) were injected for the *ex vivo* Seahorse extracellular flux assay. MM1S-luc cells (0.5×10^6) were injected for the CD38 KD xenograft. Mice injected with MM1S-luc cells were monitored via *in vivo* bioluminescent imaging (Bruker), as previously described (31). At predefined humane end points, mice were sacrificed (6–12 weeks after injection), bone marrow isolated, and engraftment determined. Human multiple myeloma cells were purified from the heterogeneous bone marrow by MACS microbeads. This purified human multiple myeloma cell population was used for the PCR and agarose gel electrophoresis. Levels of mitochondria in the purified MM1S-luc populations were achieved using MitoTracker Green FM staining and flow cytometry.

Seahorse extracellular flux assay

Oxidative phosphorylation and glycolysis rates were assessed in multiple myeloma cells using the Seahorse XFp Analyzer, as previously described (29), and the Seahorse XF Mito stress test Kit (Agilent Seahorse Bioscience), according to the manufacturer's specifications. Cocultures of primary human BMSC and multiple myeloma cells were prepared in a 1:5 ratio for 24 hours. Further information can be found in Supplementary Methods section.

Murine mitochondrial DNA detection

Murine mitochondrial DNA (mtDNA) detection was used to determine if interspecies mitochondrial transfer occurred from

murine BMSC to human multiple myeloma cells, as previously described (15). DNA from the purified human multiple myeloma cells was extracted using the GenElute mammalian DNA miniprep kit. Eight nanogram of DNA was added to the PCR reaction containing SYBR Green and murine primers provided in the Detroit R&D Kit. PCRs were amplified for 40 cycles (95°C/15 seconds, 60°C/60 seconds) on a Roche 96-well LightCycler480. PCR products were run on a 1.25% agarose gel at 100V for 1 hour. Detection was performed by Chemdoc-It2 Imager (UVP) and analyzed using ImageJ. We were able to quantify movement of mitochondria between murine bone marrow cells and human multiple myeloma cells using species specific Taqman probes purchased from ThermoFisher. These contained murine and human ND1 mitochondrial probes (on VIC and FAM fluorophores) along with murine and human TERT genomic probes. Extracted DNA was amplified for 40 cycles (95°C/15 seconds, 60°C/60 seconds) on a Roche 96-well LightCycler480. mtDNA copy numbers were determined for both human and murine mitochondria using the ΔΔCt method, using human genomic TERT to normalize results. These values were used to generate the percentage of mouse mitochondria in the human multiple myeloma cells, ultimately used to quantify mitochondrial transfer.

Confocal microscopy

To visualize tumor-derived tunneling nanotubes (TNT), BMSCs were stained with 200 nmol/L MitoTracker Green FM, and multiple myeloma cells were stained with Vybrant Dil stain to visualize cell membranes. After coculture, cells were fixed with 4% paraformaldehyde and imaged. In addition, the rLV.EF1.AcGFP-Mem9 lentivirus was purchased from Clontech Takara Bio Europe, enabling the stable tagging of plasma membranes with a GFP fluorophore. MM1S cells were transduced with this lentivirus and cultured for 72 hours prior to use. BMSCs were stained with 200 nmol/L MitoTracker CMXRos and cultured with MM1S cells transduced as above for 24 hours, before fixation with paraformaldehyde. Confocal images were acquired on Zeiss LSM 800 Axio Observer.Z1 confocal microscope with a 40X water objective (Carl Zeiss) and a Zeiss AxioPlan 2ie (Carl Zeiss). The frequency of TNT formation was analyzed through quantifying TNT anchor points (TAP), on BMSC after coculture with multiple myeloma cells, per confocal image as previously described (15). TAPs were also assessed under cytochalasin B treatment and with CD38 KD multiple myeloma cell lines.

Results

Multiple myeloma metabolic plasticity

To determine the role of the BMM on metabolism of malignant plasma cells, we analyzed the metabolic output [oxygen consumption rate (OCR) and extracellular acidification rate] of primary multiple myeloma cells, at point of isolation from the human bone marrow, and compared this with multiple myeloma cell lines grown in culture. Figure 1A and B shows that primary multiple myeloma cells ($n = 4$) have increased mitochondrial-based metabolism compared with cell lines ($n = 4$). The levels of glycolysis, measured by extracellular acidification, are lower in primary multiple myeloma compared with multiple myeloma cell lines (Fig. 1C). To further investigate this difference *in vivo*, we compared the OCR and lactate levels in MM1S cells cultured *in vitro* with MM1S cells after engraftment in NSG mice. We found increased mitochondrial-based metabolism in the MM1S isolated from the mouse compared with the cells grown *in vitro* (Fig. 1D and E), with no difference observed in glycolysis levels (Fig. 1F). Next, we compared the bioenergetics of multiple myeloma cell lines grown alone or with primary BMSCs. Increased mitochondrial metabolism was observed in cell lines cultured with BMSC compared with cell lines cultured alone (Fig. 1G–I). Finally, we show that multiple myeloma cell lines have increased ATP production and proliferation when cultured with BMSC (Fig. 1J).

To determine whether the increase in mitochondrial metabolism is due to the direct contact between BMSC and multiple myeloma cells, we repeated the Seahorse extracellular flux assay with multiple myeloma cells cultured for 24 hours in BMSC conditioned medium ±0.2 μmol/L filtration. The increased mitochondrial metabolism and increase in ATP production are not observed in multiple myeloma cultured in BMSC conditioned medium (Fig. 1K and L), highlighting the need for direct contact between BMSC and multiple myeloma cells for the bioenergetic effect observed. To further examine this process, we treated BMSC with 25 μmol/L Rotenone to inhibit BMSC mitochondria. Figure 1M presents that multiple myeloma cells cultured on Rotenone-treated BMSC have lower levels of mitochondrial respiration. Furthermore, the addition of dimethyl succinate directly to multiple myeloma cells (without BMSC) had no effect on OCR (Supplementary Fig. S1A). This shows that the mitochondrial metabolic status of BMSC plays a role in the bioenergetic flexibility in multiple myeloma cells after culture with BMSC. Furthermore, we isolated mitochondria from BMSC and multiple myeloma cells and analyzed the levels of OCR. We found BMSC mitochondria to have a 10-fold increase in OCR compared with multiple myeloma cells, highlighting that BMSC mitochondria are more functional (Supplementary Fig. S1B). Finally, we examined the effect of 10 mmol/L glucose, compared with 2.5 mmol/L, on mitochondrial respiration in multiple myeloma cells. Figure 1N shows that the same increase in mitochondrial respiration is observed between the two glucose conditions.

Mitochondria are transferred from BMSC to multiple myeloma cells

To understand how multiple myeloma can switch on oxidative phosphorylation when in the presence of BMSC, we explored the possible transfer of mitochondria from BMSC to multiple myeloma. The transfer of mitochondria from nonmalignant cells of the tumor microenvironment to malignant cells has recently been reported in a number of cancers including acute myeloid leukemia and melanoma (9, 11, 12, 15, 16). To determine if multiple myeloma acquire mitochondria from BMSC to support oxidative phosphorylation, we employed three methods. First, we used a MitoTracker mitochondrial transfer assay (15), where both BMSC and multiple myeloma cells are stained with MitoTracker and cultured together, and any increase in MitoTracker fluorescence after coculture in tumor cells shows mitochondrial transfer has occurred. Primary multiple myeloma samples ($n = 10$) cultured on BMSC have increased MitoTracker levels compared with monocultured multiple myeloma cells (Fig. 2A). This is also the case for 4 of 5 multiple myeloma cell lines tested, MM1S, U266, RPMI, and H929, shown in Fig. 2B. Second, we infected primary BMSC with an rLV.EF1.mCherry lentivirus for stable production of mitochondria-incorporated mCherry-tagged protein. Figure 2C shows upon the culture of multiple myeloma cell lines on these infected BMSC, the multiple myeloma acquires the mCherry fluorescence.

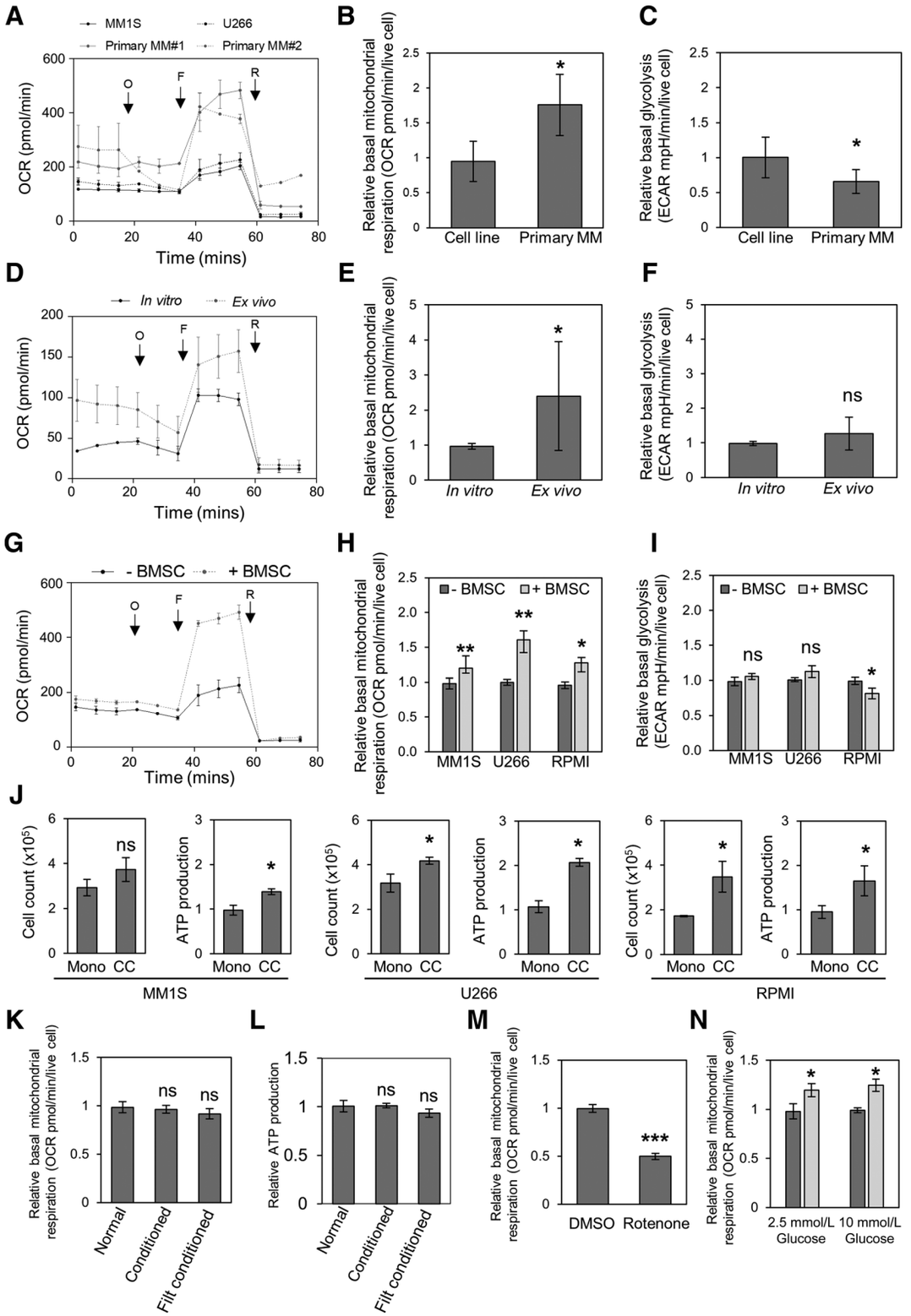

Figure 1.

Multiple myeloma (MM) favors oxidative phosphorylation in the presence of the BMM. Primary multiple myeloma cells were analyzed using the Seahorse extracellular flux assay with Mito Stress kit. All Seahorse extracellular flux experiments were carried out in Seahorse conventional (*Continued on the following page.*)

Finally, we used an *in vivo* model to determine if mitochondrial transfer occurs within the malignant BM. To do this, MM1S and U266 multiple myeloma cell lines were engrafted into NSG mice, and following tumor engraftment, we isolated the human multiple myeloma cells and determined if mouse mtDNA could be detected in human multiple myeloma cells after extraction from mouse BM. We transplanted 3 animals with MM1S and 3 with U266 multiple myeloma cells, all animals engrafted with the multiple myeloma cell line (Supplementary Fig. S2A). Human multiple myeloma cells were sorted from mouse bone marrow cells, achieving a 98.53% human population (Supplementary Fig. S2B). We extracted DNA from the purified multiple myeloma population and performed a PCR analyzing mouse mitochondrial DNA and mouse genomic DNA. Figure 2D shows that multiple myeloma cells isolated from engrafted NSG mice contained mouse mitochondrial DNA but not mouse genomic DNA.

To determine whether the mitochondria that enter the malignant plasma cells are functional, we treated multiple myeloma cell lines and primary multiple myeloma cells ($n = 5$) with rotenone to inhibit mitochondrial function and assess whether function can be restored by coculture with BMSC. Figure 2E shows that primary multiple myelomas have reduced tetramethylrhodamine, methyl ester (TMRM) fluorescence when treated with rotenone, but this is prevented when cultured on BMSC. Figure 2F shows that TMRM fluorescence is higher in rotenone-treated multiple myelomas that have been cultured with BMSC compared with monoculture. Because oxidative stress increases mitochondrial transfer from nonmalignant cells to malignant cells (15) and chemotherapy treatment induces oxidative stress, we wanted to determine if the multiple myeloma chemotherapy drug, bortezomib, increased mitochondrial transfer. We found that the addition of bortezomib to the coculture, between BMSC and primary multiple myeloma cells ($n = 7$), increased mitochondrial transfer (Fig. 2G). This was also the case in four multiple myeloma cell lines, where mitochondrial transfer was increased (Fig. 2H).

In addition, we quantified the levels of transfer *in vitro* using qPCR with species-specific Taqman probes. We cultured human multiple myeloma cell lines with the murine BMSC cell line M2-10B4 for 24 hours, extracted DNA, and carried out a qPCR with probes designed to detect human and murine ND1. We found 3% of the total mitochondria in the human multiple myeloma cell to be of mouse origin (Supplementary Fig. S3A). Finally, to demonstrate that the 3% of transferred mitochondria are having significant effects on multiple myeloma cell OXPHOS, we generated rho0 BMSC (Supplementary Fig. S3B) and cultured multiple myeloma cells on both rho0 BMSC and control BMSC. Figure 2I shows that multiple myeloma cells cultured on rho0 BMSC have lower levels of mitochondrial respiration (basal and maximal) compared with multiple myeloma cells cultured on control BMSC.

Mitochondrial transfer in multiple myeloma is via TNTs

Mitochondria have been reported to move via both TNTs (10, 15, 32) and endocytosis (16). To understand how mitochondria move to multiple myeloma, we used TNT and endocytosis inhibitors, cytochalasin B and dansylcadavarine, respectively. Cytochalasin B reduced mitochondrial transfer to multiple myeloma cell lines by up to 46.19% (Fig. 3A), whereas there was no significant reduction observed with dansylcadavarine (Fig. 3B). We also found no mitochondrial transfer occurred from BMSC to malignant plasma cells when multiple myelomas were cultured in a transwell system (Supplementary Fig. S4). Next, we used fixed cell confocal microscopy to visualize the highly dynamic TNTs. To do this, we stained multiple myeloma cells with the Vybrant lipid stain (red) and the mitochondria in BMSC with MitoTracker Green stain and then cultured the cells together for 24 hours. Following coculture, the cells were fixed and TNT formation was detected using confocal microscopy. We observed red TNTs formed between BMSC and the multiple myeloma cell line MM1S (Fig. 3C) and green mitochondria from the BMSC located in the MM1S cells. In addition, we stably expressed GFP in the plasma membrane of multiple myeloma cells, using a lentivirus, and cultured them with MitoTracker Red CMXRos. We visualized green TNTs between multiple myeloma cells and BMSC, using fixed cell confocal microscopy, with red mitochondria within the nanotube (Fig. 3D and E). Using this method, we found approximately 60% of the multiple myeloma cells had visible TNT projections (Supplementary Fig. S5A).

To quantify the number of TNTs formed during a coculture, we used TAPs and confocal microscopy, as previously described (15). TAPs are residual plasma cell–derived Vybrant DiI stains that remain on BMSC after TNT contact. TAPs can be observed in cocultures of multiple myeloma cells and BMSC (Fig. 3F). We show that TAPs can also be visualized between GFP plasma membrane–tagged multiple myeloma cells and MitoTracker CMXRos–stained BMSC (Supplementary Fig. S5B and S5C). Quantification of TAPs in four multiple myeloma cell lines shows a median of 232.5 (range, 218–278)—TAPs per confocal image (Supplementary Fig. S6). Upon cytochalasin B treatment, the number of TAPs was significantly reduced (median reduction, 75.09%; range, 71.3%–79.27%; Fig. 3G). No TAPs are formed when multiple myeloma cells are cultured in a transwell system or when medium from Vybrant DiI–stained multiple myeloma cells is added to BMSC, therefore confirming that TAPs are only present when the two cell types are in direct contact (Supplementary Fig. S7).

(*Continued.*) Mitostress base media containing 2.5/10 mmol/L glucose, 2 mmol/L glutamine, and 1 mmol/L pyruvate. **A,** OCR of two primary multiple myeloma cells and two multiple myeloma cell lines is presented. **B,** Basal mitochondrial respiration of multiple myeloma cell lines ($n = 4$) vs. primary multiple myeloma cells ($n = 4$). **C,** Basal glycolysis rates of multiple myeloma cell lines ($n = 4$) vs. primary multiple myeloma cells ($n = 4$). **D–F,** MM1S-luc cells were injected in NSG mice ($n = 6$), and 2 weeks after injection, the multiple myeloma cells were sorted from the mouse bone marrow. **D,** OCR of MM1S cells grown *in vitro* and MM1S cells isolated from mice. Basal mitochondrial respiration (**E**) and glycolysis rates (**F**) of MM1S cells grown *in vitro* and MM1S cells isolated from mice. **G–I,** Multiple myeloma cell lines were grown with and without BMSC for 72 hours, and multiple myeloma cells were then analyzed by Seahorse. **G,** OCR of MM1S cells grown with and without BMSC. Basal mitochondrial respiration (**H**) and glycolysis rates (**I**) of MM1S, U266, and RPMI grown with and without BMSC. **J,** Growth capacity and ATP production were measured in MM1S, U266, and RPMI grown with and without BMSC for 72 hours. **K** and **L,** Multiple myeloma cells were cultured in BMSC conditioned medium ± 0.2 μm filtration for 24 hours, followed by Seahorse extracellular flux analysis (**K**) or CellTitre-Glo ATP analysis (**L**). **M,** BMSCs were treated with 25 μmol/L rotenone or DMSO for 30 minutes before coculture with multiple myeloma cells. Mitochondrial respiration was measured in multiple myeloma using the Seahorse extracellular flux assay. **N,** The Seahorse extracellular flux assay in **H** was repeated in 10 mmol/L glucose MitoStress conventional base medium. ns, nonsignificant; *, $P < 0.05$; **, $P < 0.01$; ***, $P \leq 0.001$.

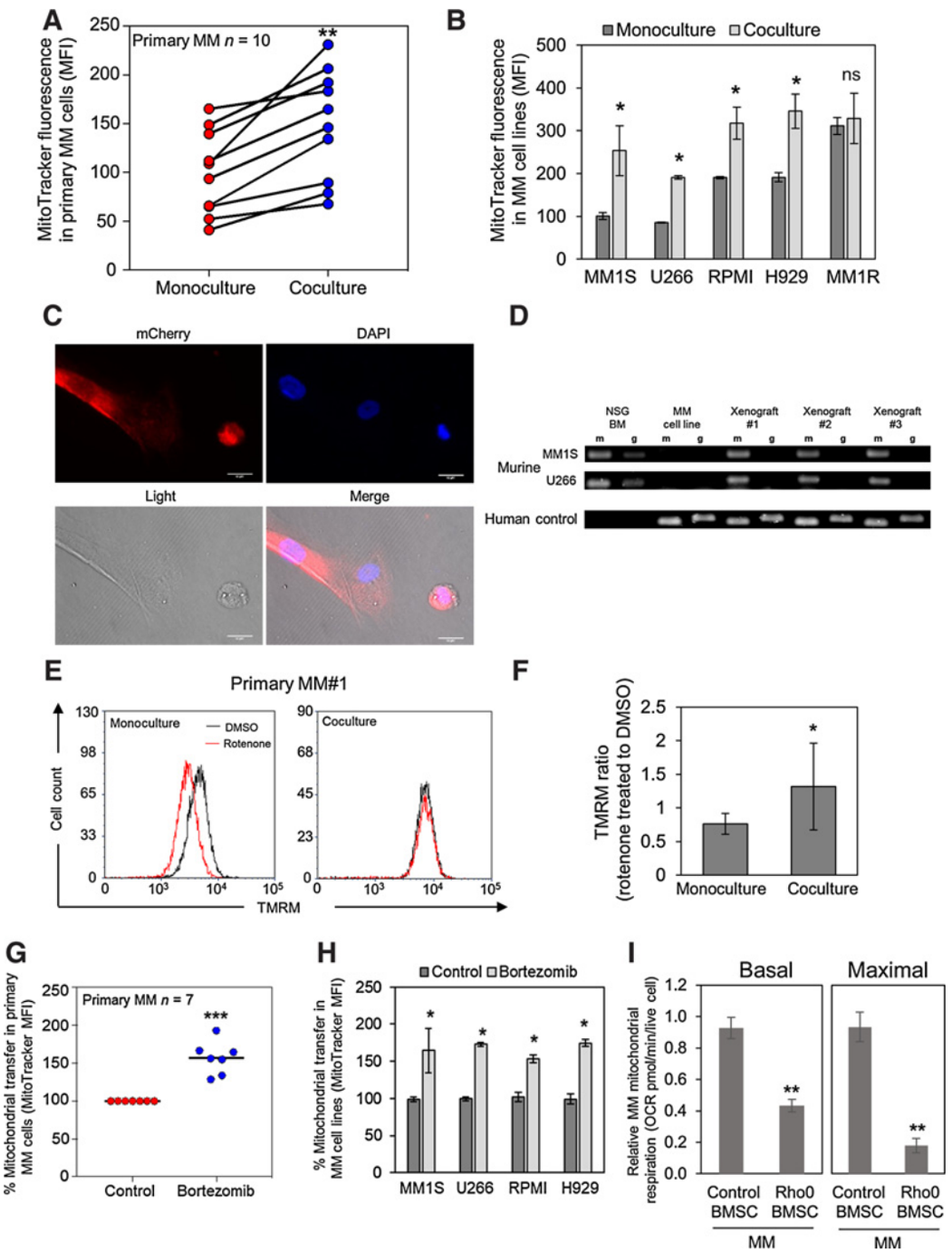

Figure 2.

Mitochondria are transferred from BMSC to multiple myeloma (MM) cells *in vitro* and *in vivo*. Primary multiple myeloma cells ($n = 10$; **A**) or multiple myeloma cell lines ($n = 5$; **B**) were prestained with 200 nmol/L MitoTracker Green FM and were cultured for 24 hours on BMSC stained with MitoTracker Green FM. MitoTracker fluorescence was analyzed in the multiple myeloma cells by flow cytometry. **C,** RPMI multiple myeloma cell line was grown on rLV.EF1.mCherry BMSC, and mCherry acquisition by multiple myeloma cells was detected by fluorescent microscopy. **D,** NSG mice were injected with either MM1S-luc cells or U266-Luc cells. Two weeks after engraftment, multiple myeloma cells were isolated from the BM, and total DNA was extracted from the purified multiple myeloma populations and analyzed by PCR for murine and human-specific mitochondrial and genomic DNA. PCR products were visualized by agarose gel electrophoresis. **E,** Primary MM#1 was treated with 25 μmol/L rotenone or DMSO for 15 minutes and then washed and cultured with or without BMSC. Multiple myeloma cells were then stained with 30 nmol/L TMRM for 15 minutes before flow cytometry analysis. Representative flow cytometry plots are presented. **F,** Primary multiple myeloma and multiple myeloma cell lines ($n = 5$) were treated as in **E**, and TMRM ratio of rotenone/DMSO of multiple myeloma cells grown with and without BMSC is presented. **G** and **H,** Mitochondrial transfer levels were assessed, using MitoTracker Green, from BMSC to primary multiple myeloma cells ($n = 7$; **G**) or multiple myeloma cell lines ($n = 4$; **H**) upon the addition of 10 nmol/L bortezomib. **I,** Rho0 BMSCs were generated from the BMSC cell line HS-5. Multiple myeloma primary cells were then grown on control BMSC or rho0 BMSC for 48 hours, and multiple myeloma cells were then analyzed by Seahorse for OCR at basal and maximal conditions. ns, nonsignificant; *, $P < 0.05$; **, $P < 0.01$; ***, $P \leq 0.001$.

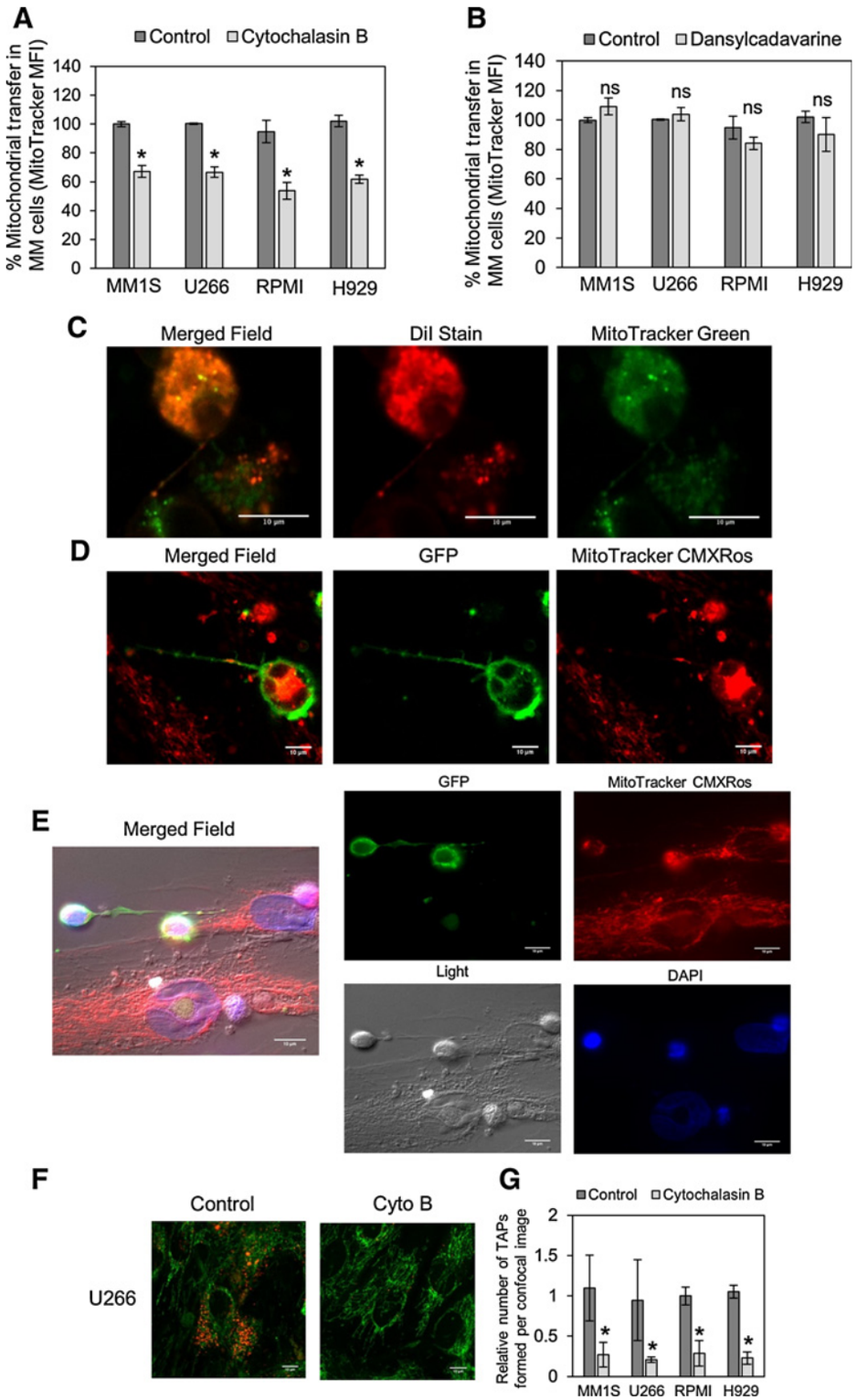

Figure 3.

Mitochondrial transfer in multiple myeloma is via TNTs. Multiple myeloma cell lines and BMSC were prestained with 200 nmol/L MitoTracker Green for 1 hour and then cultured together before 24-hour drug treatment, with 350 μmol/L cytochalasin B (**A**) and 50 μmol/L dansylcadavarine (**B**). Flow cytometry was used to detect MitoTracker Green FM in the multiple myeloma cells. **C,** MM1S cells were stained with Vybrant DiI for 1 hour and washed three times in PBS. BMSCs were stained with MitoTracker Green FM for 1 hour and washed three times in PBS. Multiple myeloma cells and BMSCs were then cocultured for 24 hours before fixation using paraformaldehyde. Cells were visualized by confocal microscopy. **D** and **E,** MM1S cells lentivirally transduced with the rLV.EF1.AcGFP-Mem9 virus were cultured with BMSC stained with MitoTracker CMXRos for 24 hours before fixation with paraformaldehyde. Confocal microscopy imaging highlighted TNTs formed between the multiple myeloma and BMSC. **F,** U266 multiple myeloma cells and BMSC were prepared and cultured as in **C**. U266 multiple myeloma cells were washed off prior to fixation. TAPs on BMSC were visualized by confocal microscopy and quantified on each confocal image obtained ($n = 5$). **G,** This was carried out also for multiple myeloma cell lines MM1s, RPMI, and H929. ns, nonsignificant; *, $P < 0.05$.

CD38 inhibition prevents mitochondrial transfer and TNT formation

Hayakawa and colleagues recently reported that mitochondria are released by astrocytes as mitochondria-containing particles, in a CD38-dependent process, and recaptured by neurons (18). Studies have shown that CD38 expression in multiple myeloma is high compared with nonmalignant plasma cells (33). Therefore, we correlated the CD38 expression levels to mitochondrial

transfer levels of the multiple myeloma cell lines and primary multiple myeloma cells ($n = 12$). We found there to be a strong correlation ($R = 0.7915$; $P = 0.0013$; Fig. 4A). Using a CD38-blocking antibody, mitochondrial transfer to primary multiple myeloma is significantly reduced ($n = 8$; Fig. 4B). Knockdown of CD38 in the multiple myeloma cell lines, MM1S, U266, RPMI, and H929 (Fig. 4C; Supplementary Fig. S8), reduced mitochondrial transfer from BMSC to multiple myeloma (Fig. 4D). We next analyzed the cell viability and levels of apoptosis in CD38 KD and control KD cells cultured with BMSC. We found there to be decreased cell viability and increased levels of apoptosis in CD38 KD cells compared with control KD cells (Fig. 4E and F).

A recent study identified that all-trans retinoic acid (ATRA) increases CD38 expression on acute myeloid leukemia (34). We next identified if this was the case for multiple myeloma. Figure 4G and H shows CD38 is upregulated in multiple myeloma cells after 1 μmol/L ATRA treatment both at RNA and protein levels. We tested whether this increase in CD38 induces mitochondrial transfer, and Fig. 4I shows that this is the case with increased levels of mitochondrial transfer found in three multiple myeloma cells lines tested. Taken together, these results show functionally that mitochondrial transfer from BMSC to multiple myeloma cells requires CD38 and supports multiple myeloma growth and survival.

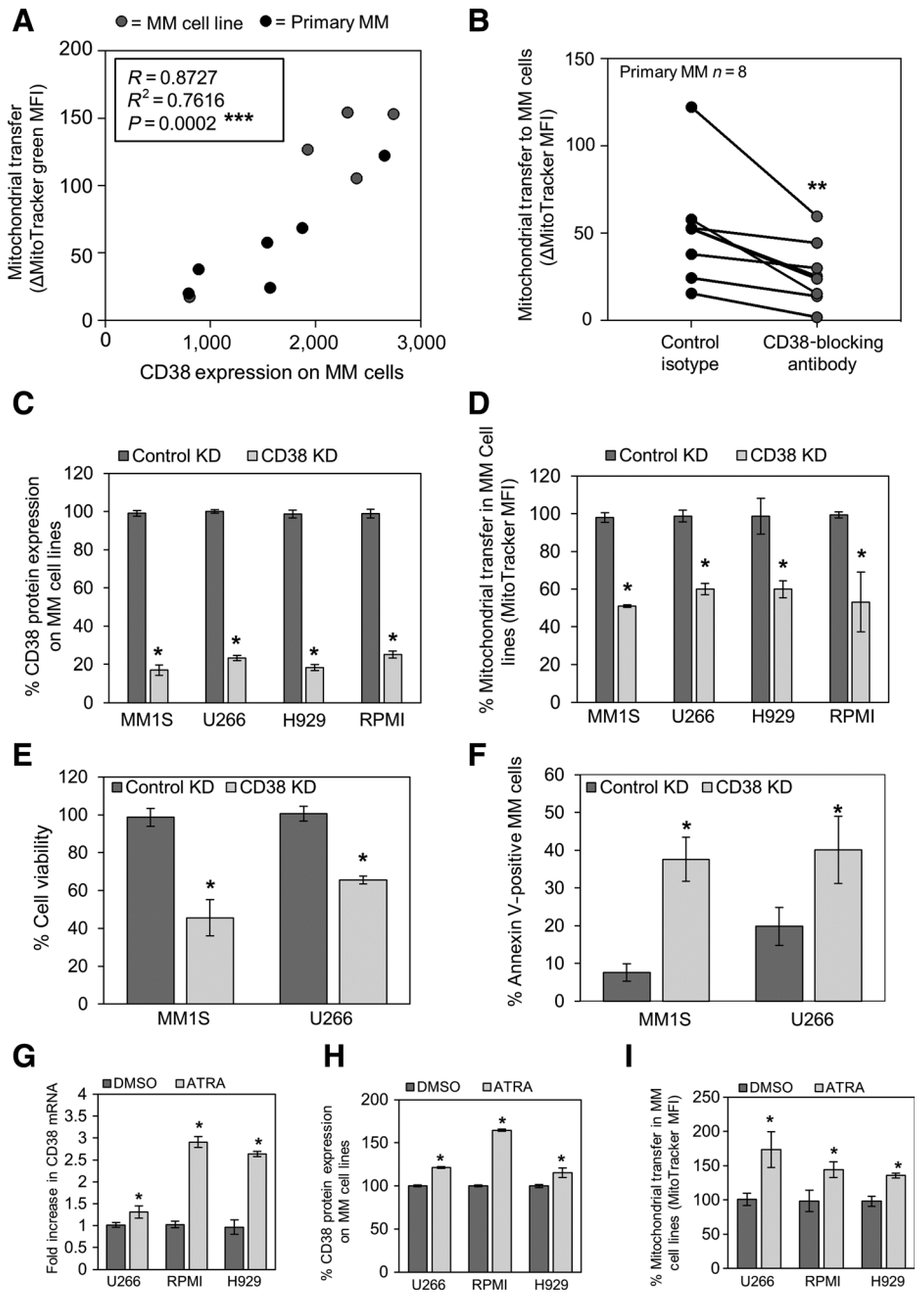

Figure 4.

CD38 inhibition prevents mitochondrial transfer and TNT formation. **A,** Mitochondrial levels in primary multiple myeloma (MM) cells ($n = 7$) and multiple myeloma cell lines ($n = 5$) were correlated to CD38 expression on these cells. Mitochondrial levels were achieved using the MitoTracker-based assay, whereas CD38 expression was determined using flow cytometry. **B,** Primary multiple myeloma cells ($n = 8$) and BMSC were prestained with 200 nmol/L MitoTracker Green for 1 hour and then cultured together before 24-hour treatment with a CD38-blocking antibody. Flow cytometry was used to detect MitoTracker Green FM in the multiple myeloma cells. **C,** Four multiple myeloma cell lines were transduced with a lentivirus targeted to CD38 or control for 72 hours. CD38 protein expression levels were analyzed by flow cytometry. **D,** The four multiple myeloma cell lines transduced with a lentivirus targeted to CD38 or control were prestained, along with BMSC, with MitoTracker Green for 1 hour and then cultured together for a further 24 hours before MitoTracker was assayed by flow cytometry. **E** and **F,** Control KD and CD38 KD MM1S and U266 cells were cocultured with BMSC for 24 hours. Cell viability and levels of apoptosis were assessed using CellTitre-Glo and Annexin V staining, respectively. **G** and **H,** U266, RPMI, and H929 cells were treated with 1 μmol/L ATRA or DMSO overnight. CD38 expression was analyzed in multiple myeloma cells at RNA (**G**) and protein (**H**) levels using qPCR and flow cytometry, respectively. **I,** Mitochondrial transfer levels from BMSC to multiple myeloma cells were analyzed using the MitoTracker Green mitochondrial transfer assay after treatment of multiple myeloma cells with ATRA. *, $P < 0.05$; **, $P < 0.01$.

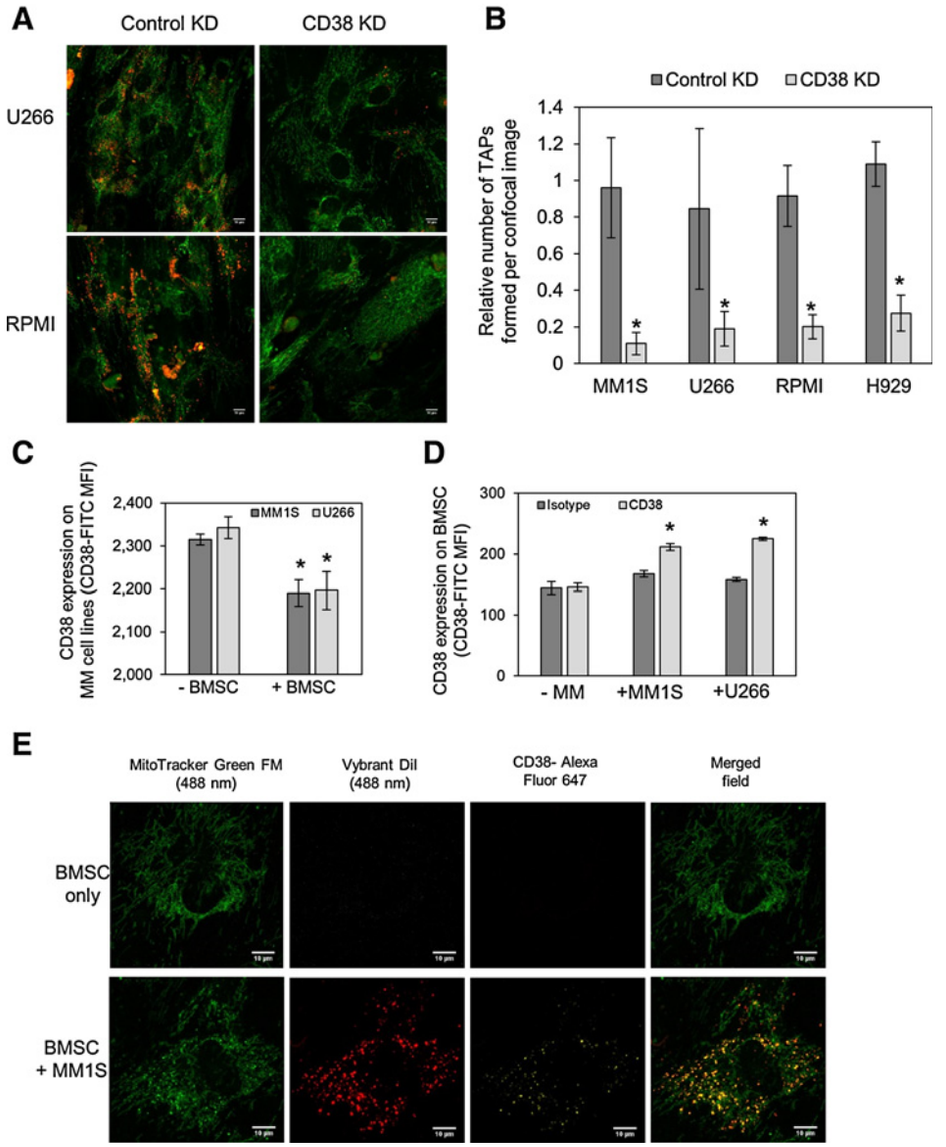

Figure 5.
Tumor cell CD38 supports the formation of TNTs. **A,** MM1S, U266, RPMI, and H929 multiple myeloma (MM) cell lines, transduced with a lentivirus targeted to CD38 or control, were stained with Vybrant Dil for 1 hour and washed three times in PBS. BMSCs were stained with MitoTracker Green FM for 1 hour and washed three times in PBS. Multiple myeloma cells and BMSCs were then cocultured for 24 hours, and multiple myeloma cell lines were removed before fixation using paraformaldehyde. TAPs were visualized on BMSC by confocal microscopy. **B,** TAPs formed by control KD and CD38 KD cells were quantified on BMSC using confocal images obtained ($n = 5$). **C** and **D,** MM1S and U266 multiple myeloma cell lines were cocultured with BMSC for 24 hours. Cells were removed and analyzed for CD38 expression by flow cytometry. **E,** The location of CD38 on BMSC, after TAP formation by MM1S cells, was determined by staining with a CD38 antibody (Alexa Fluor 647). TAPs and CD38 expression were visualized on BMSC by confocal microscopy. *, $P < 0.05$.

Tumor cell CD38 supports the formation of TNTs

CD38 is known to facilitate the adhesion of leukocytes to endothelial cells (35); therefore, we hypothesized that CD38 has a role in the formation of the TNT. TAP quantification was used in cocultures between BMSC and control KD or CD38 KD multiple myeloma cell lines. Figure 5A shows reduced TAP formation by U266 and RPMI in CD38 KD cells. This result is replicated with MM1S and H929 multiple myeloma cell lines (Fig. 5B). Observations show that TAP formation leaves some residual multiple myeloma cell membranes on the BMSC. To determine if multiple myeloma–derived CD38 is part of this residual membrane that is left on the BMSC after TAP formation, flow cytometry was used to detect CD38 expression on multiple myeloma and BMSC before and after coculture. Figure 5C shows that CD38 expression is lower on multiple myeloma after coculture with BMSC, whereas CD38 can be detected on BMSC after multiple myeloma coculture (Fig. 5D). Figure 5E shows that CD38 localizes to TAPs on BMSC after coculture with multiple myeloma.

Targeting CD38 *in vivo* blocks mitochondrial transfer and improves animal survival

To determine the *in vivo* significance of CD38 inhibition on mitochondrial transfer, we engrafted control KD and CD38 KD MM1S-luc cells into NSG mice. Multiple myeloma disease progression in these mice was analyzed weekly by live animal bioluminescence, which revealed that there was consistently reduced tumor burden in the bone marrow with CD38 KD cells (Fig. 6A). Survival of mice transplanted with CD38 KD cells had a significantly increased survival time compared with control KD cells (Fig. 6B) but no difference in the growth capability when cultured *in vitro* (Fig. 6C). Analysis of the BM confirmed engrafted into NSG mice (Supplementary Fig. S9).

To determine if mitochondrial transfer was affected by CD38 KD, we assessed the levels of mitochondria after engraftment in the human multiple myeloma cell population, using MitoTracker Green staining. Multiple myeloma cells after engraftment have significantly reduced mitochondrial levels in CD38 KD cells

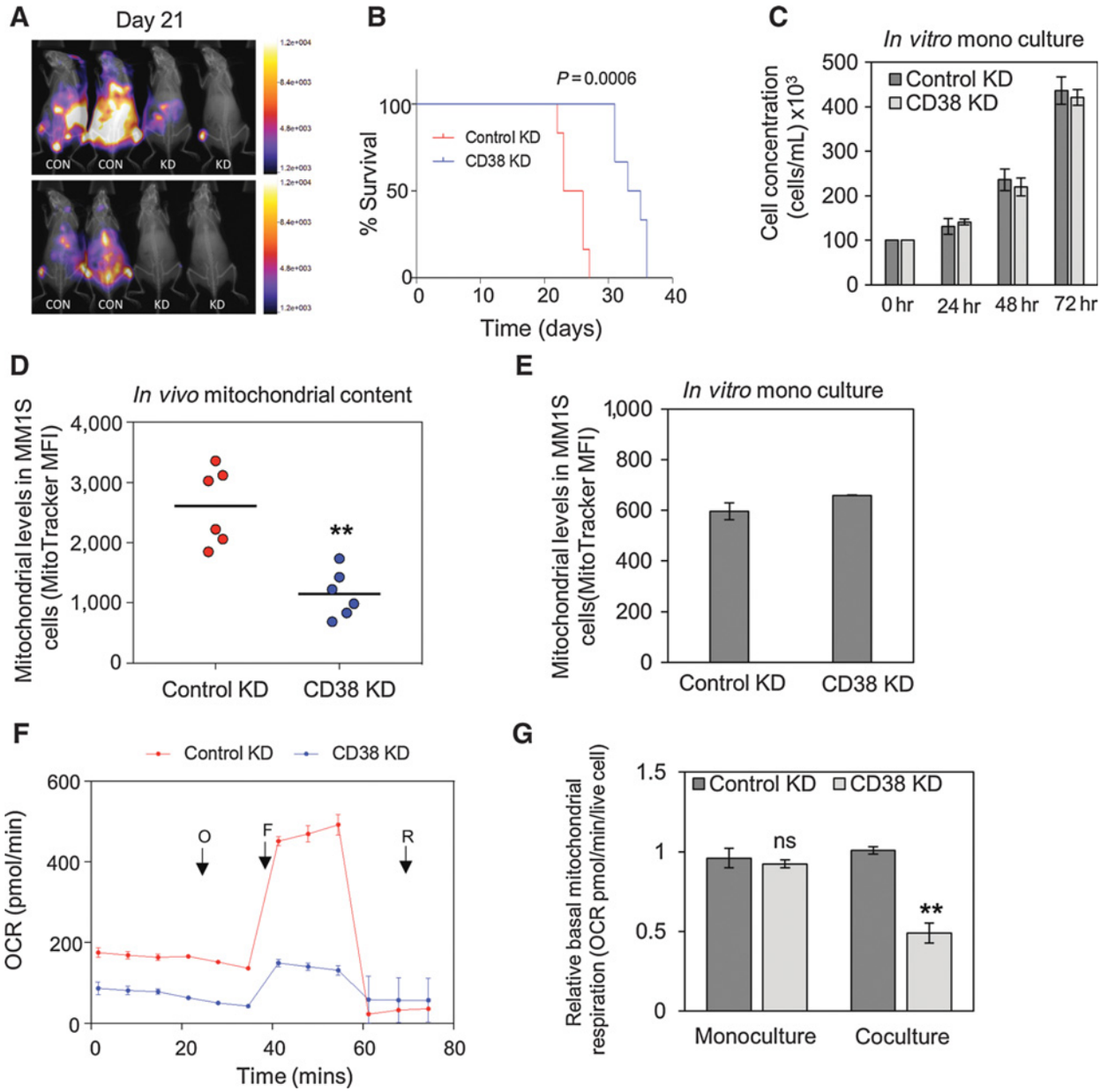

Figure 6.

Targeting CD38 *in vivo* blocks mitochondrial transfer and improves animal survival. **A,** Mice were imaged using bioluminescence weekly to monitor engraftment and disease progression in the animals injected with control and CD38 KD MM1S-luc cells. **B,** The survival of NSG mice injected with either control KD or CD38 KD MM1S-luc cells. **C,** Control KD and CD38 KD MM1S-luc cells were plated at a concentration of 100 $\times$ 10^3 cells/mL. The growth capacity of both cell types was monitored over a 72-hour period using trypan blue exclusion. **D,** Mitochondrial levels were analyzed in the purified control KD and CD38 KD multiple myeloma cells, after isolation from recipient animals, by staining for 15 minutes in 200 mmol/L MitoTracker Green and flow cytometry. **E,** Mitochondrial levels in control KD and CD38 KD multiple myeloma cells cultured *in vitro* were analyzed by MitoTracker fluorescence. **F,** CD38 KD and control KD MM1S cells were grown *in vitro* with and without BMSC for 72 hours prior to analysis by the Seahorse extracellular flux analyzer with MitoStress kit. **G,** OCR of CD38 KD and control KD MM1S cultured with BMSC. Data represented as mean $\pm$ SD. **F,** Basal mitochondrial respiration of CD38 KD and control KD MM1S cells grown with and without BMSC. ns, nonsignificant; **, $P < 0.01$.

compared with control KD cells; however, no difference was observed when cultured *in vitro* (Fig. 6D and E). Finally, we measured the mitochondrial respiration rates in CD38 KD MM1S cells grown *in vitro* with and without BMSC. Figure 6F and G shows that there is significant reduction in mitochondrial respiration in CD38 KD cells grown with BMSC compared with control KD cells. No difference in mitochondrial respiration was observed between CD38 KD and control KD cells grown without BMSC. These

results identify *in vivo* a functional, protumoral role for CD38-driven mitochondrial transfer in multiple myeloma.

Discussion

The biological phenomenon of mitochondrial trafficking between nonmalignant cells and malignant cells is increasingly becoming recognized as part of the cancer phenotype. This process provides the oxidative phosphorylation machinery to enable increased ATP production to aid cancer progression. Here, we examine the metabolic changes resultant from mitochondrial transfer in multiple myeloma, which to date has been regarded as a glycolytic tumor (3–5).

In this study, we investigate the influence of the BM on the energy output of multiple myeloma. Multiple myeloma cells are known to generally use the nonmitochondrial-based process of glycolysis to generate its ATP and have been shown to be susceptible to glycolysis inhibitors (3, 5), and these studies have only focused on multiple myeloma cell lines not in the presence of their protective microenvironment. The study by Dalva-Aydemir and colleagues shows that multiple myeloma cell lines have the capability of undergoing functional oxidative phosphorylation after treatment with the glycolysis inhibitor ritonavir (5). Further data proposing a reliance on glycolysis in multiple myeloma were provided by Fujiwara and colleagues (2013) who showed increased expression of genes associated with a glycolytic profile in primary multiple myeloma. Moreover, others have shown that PET imaging can be used in the diagnosis of myeloma, and results show that high glucose uptake is associated with poor prognosis (36, 37). In our study, we show that multiple myeloma within the BMM utilizes oxidative phosphorylation and glycolysis to provide the necessary energy for survival and proliferation. Interestingly, others have shown that glucose can feed the TCA cycle via circulating lactate derived from glycolysis (38). Moreover, the authors of this article show that lactate (derived from glycolysis) is a primary TCA substrate in lung tumors. Another study shows that lactate can feed the TCA cycle in both human and mouse tumors (39). Therefore, we hypothesize based on these reports and data from our own experiments that in myeloma (and potentially other tumors) glucose is used by glycolysis (PET scan positive); the metabolite, lactate, is then fed into the TCA cycle to generate ATP by oxidative phosphorylation in the presence of functional mitochondria, which have been derived from the BMSCs.

We demonstrate that mitochondrial trafficking from BMSC to multiple myeloma orchestrates this plasticity in multiple myeloma metabolism. Cytochalasin B (which inhibits TNT formation) reduced mitochondrial transfer to multiple myeloma cell lines by approximately one half, establishing mechanistically that multiple myeloma can be added to an emerging list of tumors that are capable of acquiring mitochondria from neighboring nonmalignant cells through TNTs (11, 15, 22, 32). Furthermore, transferred mitochondria were found to metabolically promote oxidative phosphorylation, which was functionally beneficial to the tumor and remained so in the presence of chemotherapy treatment. Protumoral mitochondrial transfer therefore can be considered part of the malignant phenotype of the disease and in addition contributes to the cancer cell survival response to chemotherapy. As the number of tumors in which this phenomenon is identified grows, it becomes increasingly likely that mitochondrial transfer through TNTs forms, more broadly, a fundamental component of a common malignant phenotype.

CD38 has a dual role as both a receptor involved in the migration of leukocytes (40) and as an ectoenzyme catalyzing the formation of ADPR from NAD^+ (41). Originally thought to be expressed only on hematopoietic and neuronal cells, CD38 is now known to be expressed on many other cell types such as prostate (42), lung (43), and skin cells (44). CD38 has recently been shown to have a role in the movement of mitochondria between astrocytes and damaged neurons after stroke (18). In this study, mitochondria were shown to move in microvesicles, which enabled the restoration of metabolic potential and survival of neurons after stroke, and this process was shown to be dependent on CD38. Others have shown that lipopolysaccharide induces mitochondrial transfer from BMSC to alveoli (17), and lipopolysaccharide can induce CD38 upregulation (45). We further present that mitochondrial transfer in multiple myeloma is via a CD38-dependant mechanism, independent of microvesicle transfer. CD38 inhibition reduced TAP formation in our study directly linking multiple myeloma nanotube attachment to nonmalignant stromal cells and tumor CD38 expression. Metabolically, we observed a significant reduction in mitochondrial respiration in CD38 KD multiple myeloma cells grown with BMSC compared with control KD cells (and this was only seen when cells were cocultured with stromal cells rather than monoculture). Functionally, *in vivo* CD38 KD improved animal survival and tumor cells from CD38 KD multiple myeloma contained significantly fewer mitochondria. These data establish that mitochondrial transfer in multiple myeloma is biologically and metabolically relevant and furthermore leads us to hypothesize that similar CD38-driven mitochondrial transfer may be relevant in other malignancies. Presently, it remains unexplained whether mitochondrial transfer occurs through CD38 activity as a cell surface receptor or ectoenzyme or through a hitherto unknown function of CD38.

Drugs targeting CD38 have recently been shown to be well tolerated and clinically efficacious in early phase studies of the treatment of relapsed refractory multiple myeloma (23). Preclinical studies found that the anti-CD38 antibody daratumumab mediates multiple myeloma cytotoxicity in the presence of the protective bone marrow, via immune-mediated killing, either antibody-dependent cell-mediated cytotoxicity or complement-dependent cytotoxicity (21, 22). As daratumumab also down-regulates $CD38^+$ regulatory T and B cells, a combination with immunomodulatory drugs has been postulated to be advantageous. The use of daratumumab-containing treatment combinations has shown significant clinical benefit in patients with both previously untreated and relapsed multiple myeloma (24–26). Although we have not tested daratumumab in this study, our results provide an alternative mechanism of action of drugs targeting CD38, showing that inhibiting CD38 can reduce mitochondrial transfer. Inhibition of mitochondrial transfer also significantly reduces the mitochondrial oxidative metabolism in the multiple myeloma cell when cultured with BMSC. We show in mouse models that multiple myeloma disease progression is reduced when CD38 is knocked down in multiple myeloma cells, and we assign this phenotype in part to reduced mitochondrial transfer levels. Moreover, to overcome multiple myeloma relapse following the use of chemotherapy agents such as bortezomib, we propose the testing of combinations of drugs targeting CD38 with established chemotherapy agents including cytotoxics and

proteasome inhibitors. If anthracyclines and proteasome inhibitors are known to induce mitochondrial transfer, then conceptually anti-CD38 therapy may work well as an adjunct in multiagent combinations.

For mitochondrial transfer to be targeted therapeutically in the clinic, viable molecular targets involved in the transfer process need to be elucidated. We recently identified that NOX2-derived superoxide from acute myeloid leukemia is crucial for mitochondrial transfer to occur in this malignancy (15). However, inhibitors of NOX2 are not clinically available, and moreover, toxicity may present a problem with such a strategy as deletion of NOX2 in humans frequently leads to death in the first decade of life (46). Here, our results identify CD38 as a viable molecular target to reduce mitochondrial transfer between nonmalignant and malignant cells, with drugs presently available for use and/or in advanced stages of preclinical development. With CD38 expression now known on a wide variety of malignant cells (47), our data lead us to hypothesize that CD38 has a potential clinical role in other cancers with mitochondrial transfer systems. Furthermore, we should look to identify alternate functional receptors in non–CD38-expressing tumors, with possible candidates including CD157, the only other known member of the CD38 superfamily.

In this study, we present a paradigm to target mitochondrial transfer as a means to perturb tumor metabolism and function as an anticancer therapeutic strategy. Here, we show that CD38 is required for the formation of TNTs facilitating protumoral mitochondrial transfer in multiple myeloma. We show increased levels of apoptosis are observed in malignant plasma cells when the number of mitochondria transferred is reduced, demonstrating this process is protumoral in multiple myeloma. Moreover, BMSC-derived mitochondria are more functional than multiple myeloma–derived mitochondria; therefore, it is metabolically advantageous to the multiple myeloma cell to acquire the BMSC mitochondria. Alternate mechanisms exist to enhance tumoral metabolic activity such as acquisition of extracellular metabolites (48). However, this does not appear to be a significant factor in multiple myeloma as in our experiments, mitochondrial respiration remained constant when metabolite containing BMSC medium was added to multiple myeloma indirectly and when dimethyl succinate was added to multiple myeloma cells independently of BMSC.

Overall, the trafficking of mitochondria allows multiple myeloma cells to switch on mitochondrial oxidative metabolism to increase ATP production. Through CD38 inhibition, mitochondrial transfer is reduced *in vitro* and *in vivo*, and multiple myeloma disease progression is reduced increasing animal survival. Drugs targeting CD38 are presently being used to treat multiple myeloma, and optimum combinations are being clinically studied. The data presented here explain that CD38 inhibition in multiple myeloma is therefore a viable treatment strategy to inhibit mitochondrial transfer for clinical benefit. Our study accordingly provides the scientific rationale and metabolic basis for inhibiting mitochondrial transfer in multiple myeloma, and we also provide a biological rationale for the selection of appropriate drugs to be used in combination with mitochondrial transfer blocking agents, and finally we propose the potential of translating these findings to other malignancies and diseases.

Disclosure of Potential Conflicts of Interest

No potential conflicts of interest were disclosed.

Authors' Contributions

Conception and design: C.R. Marlein, K.M. Bowles, S.A. Rushworth
Development of methodology: C.R. Marlein, R.E. Piddock, L. Zaitseva, K.M. Bowles, S.A. Rushworth
Acquisition of data (provided animals, acquired and managed patients, provided facilities, etc.): C.R. Marlein, R.E. Piddock, J.J. Mistry, C. Hellmich, R.H. Horton, Z. Zhou, M.J. Auger, S.A. Rushworth
Analysis and interpretation of data (e.g., statistical analysis, biostatistics, computational analysis): C.R. Marlein, J.J. Mistry, L. Zaitseva, K.M. Bowles, S.A. Rushworth
Writing, review, and/or revision of the manuscript: C.R. Marlein, K.M. Bowles, S.A. Rushworth
Administrative, technical, or material support (i.e., reporting or organizing data, constructing databases): L. Zaitseva, K.M. Bowles, S.A. Rushworth
Study supervision: K.M. Bowles, S.A. Rushworth

Acknowledgments

The authors thank the Rosetrees Trust, The Big C, and the Norwich Research Park Doctoral Training Program for funding. They also thank Professor Richard Ball, Dr. Mark Wilkinson, Iain Sheriffs, and Sue Steel, Norwich Biorepository (UK), for help with sample collection and storage. pCDH-luciferase-T2A-mCherry was kindly gifted by Professor Irmela Jeremias, MD, from Helmholtz Zentrum München, Munich, Germany. The authors also thank Allyson Tyler, Ian Thirkettle, and Karen Ashurst from the Laboratory Medicine Department at the Norfolk and Norwich University Hospital for technical assistance.

The costs of publication of this article were defrayed in part by the payment of page charges. This article must therefore be hereby marked *advertisement* in accordance with 18 U.S.C. Section 1734 solely to indicate this fact.

Received March 12, 2018; revised August 11, 2018; accepted January 3, 2019; published first January 8, 2019.

References

1. Warburg O. On the origin of cancer cells. Science 1956;123:309–14.
2. Palumbo A, Anderson K. Multiple myeloma. N Engl J Med 2011;364:1046–60.
3. Sanchez WY, McGee SL, Connor T, Mottram B, Wilkinson A, Whitehead JP, et al. Dichloroacetate inhibits aerobic glycolysis in multiple myeloma cells and increases sensitivity to bortezomib. Br J Cancer 2013;108:1624–33.
4. Fujiwara S, Kawano Y, Yuki H, Okuno Y, Nosaka K, Mitsuya H, et al. PDK1 inhibition is a novel therapeutic target in multiple myeloma. Br J Cancer 2013;108:170–8.
5. Dalva-Aydemir S, Bajpai R, Martinez M, Adekola KU, Kandela I, Wei C, et al. Targeting the metabolic plasticity of multiple myeloma with FDA-approved ritonavir and metformin. Clin Cancer Res 2015;21:1161–71.
6. Borsi E, Perrone G, Terragna C, Martello M, Dico AF, Solaini G, et al. Hypoxia inducible factor-1 alpha as a therapeutic target in multiple myeloma. Oncotarget 2014;5:1779–92.
7. Gautheron DC. Mitochondrial oxidative phosphorylation and respiratory chain: review. J Inherit Metab Dis 1984;7 Suppl 1:57–61.
8. Rustom A, Saffrich R, Markovic I, Walther P, Gerdes HH. Nanotubular highways for intercellular organelle transport. Science 2004;303:1007–10.
9. Spees JL, Olson SD, Whitney MJ, Prockop DJ. Mitochondrial transfer between cells can rescue aerobic respiration. Proc Natl Acad Sci U S A 2006;103:1283–8.
10. Lu J, Zheng X, Li F, Yu Y, Chen Z, Liu Z, et al. Tunneling nanotubes promote intercellular mitochondria transfer followed by increased invasiveness in bladder cancer cells. Oncotarget 2017;8:15539–52.

11. Pasquier J, Guerrouahen BS, Al Thawadi H, Ghiabi P, Maleki M, Abu-Kaoud N, et al. Preferential transfer of mitochondria from endothelial to cancer cells through tunneling nanotubes modulates chemoresistance. J Transl Med 2013;11:94.
12. Tan AS, Baty JW, Dong LF, Bezawork-Geleta A, Endaya B, Goodwin J, et al. Mitochondrial genome acquisition restores respiratory function and tumorigenic potential of cancer cells without mitochondrial DNA. Cell Metab 2015;21:81–94.
13. Dong LF, Kovarova J, Bajzikova M, Bezawork-Geleta A, Svec D, Endaya B, et al. Horizontal transfer of whole mitochondria restores tumorigenic potential in mitochondrial DNA-deficient cancer cells. Elife 2017;6.
14. Strakova A, Ni Leathlobhair M, Wang GD, Yin TT, Airikkala-Otter I, Allen JL, et al. Mitochondrial genetic diversity, selection and recombination in a canine transmissible cancer. Elife 2016;5.
15. Marlein CR, Zaitseva L, Piddock RE, Robinson SD, Edwards DR, Shafat MS, et al. NADPH oxidase-2 derived superoxide drives mitochondrial transfer from bone marrow stromal cells to leukemic blasts. Blood 2017;130: 1649–60.
16. Moschoi R, Imbert V, Nebout M, Chiche J, Mary D, Prebet T, et al. Protective mitochondrial transfer from bone marrow stromal cells to acute myeloid leukemic cells during chemotherapy. Blood 2016;128:253–64.
17. Islam MN, Das SR, Emin MT, Wei M, Sun L, Westphalen K, et al. Mitochondrial transfer from bone-marrow-derived stromal cells to pulmonary alveoli protects against acute lung injury. Nat Med 2012; 18:759–65.
18. Hayakawa K, Esposito E, Wang X, Terasaki Y, Liu Y, Xing C, et al. Transfer of mitochondria from astrocytes to neurons after stroke. Nature 2016;535: 551–5.
19. Siegel RL, Miller KD, Jemal A. Cancer statistics, 2016. CA Cancer J Clin 2016;66:7–30.
20. Kawano Y, Moschetta M, Manier S, Glavey S, Gorgun GT, Roccaro AM, et al. Targeting the bone marrow microenvironment in multiple myeloma. Immunol Rev 2015;263:160–72.
21. de Weers M, Tai YT, van der Veer MS, Bakker JM, Vink T, Jacobs DC, et al. Daratumumab, a novel therapeutic human CD38 monoclonal antibody, induces killing of multiple myeloma and other hematological tumors. J Immunol 2011;186:1840–8.
22. Lokhorst HM, Plesner T, Laubach JP, Nahi H, Gimsing P, Hansson M, et al. Targeting CD38 with daratumumab monotherapy in multiple myeloma. N Engl J Med 2015;373:1207–19.
23. Lonial S, Weiss BM, Usmani SZ, Singhal S, Chari A, Bahlis NJ, et al. Daratumumab monotherapy in patients with treatment-refractory multiple myeloma (SIRIUS): an open-label, randomised, phase 2 trial. Lancet 2016;387:1551–60.
24. Palumbo A, Chanan-Khan A, Weisel K, Nooka AK, Masszi T, Beksac M, et al. Daratumumab, bortezomib, and dexamethasone for multiple myeloma. N Engl J Med 2016;375:754–66.
25. Dimopoulos MA, Oriol A, Nahi H, San-Miguel J, Bahlis NJ, Usmani SZ, et al. Daratumumab, lenalidomide, and dexamethasone for multiple myeloma. N Engl J Med 2016;375:1319–31.
26. Mateos MV, Dimopoulos MA, Cavo M, Suzuki K, Jakubowiak A, Knop S, et al. Daratumumab plus bortezomib, melphalan, and prednisone for untreated myeloma. N Engl J Med 2018;378:518–28.
27. Bhatnagar V, Gormley NJ, Luo L, Shen YL, Sridhara R, Subramaniam S, et al. FDA approval summary: daratumumab for treatment of multiple myeloma after one prior therapy. Oncologist 2017;22:1347–53.
28. Piddock RE, Loughran N, Marlein CR, Robinson SD, Edwards DR, Yu S, et al. PI3Kdelta and PI3Kgamma isoforms have distinct functions in regulating pro-tumoural signalling in the multiple myeloma microenvironment. Blood Cancer J 2017;7:e539.
29. Abdul-Aziz AM, Shafat MS, Mehta TK, Di Palma F, Lawes MJ, Rushworth SA, et al. MIF-induced stromal PKCbeta/IL8 is essential in human acute myeloid leukemia. Cancer Res 2017;77:303–11.
30. Zaitseva L, Murray MY, Shafat MS, Lawes MJ, MacEwan DJ, Bowles KM, et al. Ibrutinib inhibits SDF1/CXCR4 mediated migration in AML. Oncotarget 2014;5:9930–8.
31. Vick B, Rothenberg M, Sandhofer N, Carlet M, Finkenzeller C, Krupka C, et al. An advanced preclinical mouse model for acute myeloid leukemia using patients' cells of various genetic subgroups and in vivo bioluminescence imaging. PLoS One 2015;10:e0120925.
32. Lou E, Fujisawa S, Morozov A, Barlas A, Romin Y, Dogan Y, et al. Tunneling nanotubes provide a unique conduit for intercellular transfer of cellular contents in human malignant pleural mesothelioma. PLoS One 2012;7: e33093.
33. Almeida J, Orfao A, Ocqueteau M, Mateo G, Corral M, Caballero MD, et al. High-sensitive immunophenotyping and DNA ploidy studies for the investigation of minimal residual disease in multiple myeloma. Br J Haematol 1999;107:121–31.
34. Buteyn NJ, Fatehchand K, Santhanam R, Fang H, Dettorre GM, Gautam S, et al. Anti-leukemic effects of all-trans retinoic acid in combination with Daratumumab in acute myeloid leukemia. Int Immunol 2018;30:375–83.
35. Newman PJ. Switched at birth: a new family for PECAM-1. J Clin Invest 1999;103:5–9.
36. Dammacco F, Rubini G, Ferrari C, Vacca A, Racanelli V. (1)(8)F-FDG PET/CT: a review of diagnostic and prognostic features in multiple myeloma and related disorders. Clin Exp Med 2015;15:1–18.
37. Cavo M, Terpos E, Nanni C, Moreau P, Lentzsch S, Zweegman S, et al. Role of (18)F-FDG PET/CT in the diagnosis and management of multiple myeloma and other plasma cell disorders: a consensus statement by the International Myeloma Working Group. Lancet Oncol 2017;18:e206–e17.
38. Hui S, Ghergurovich JM, Morscher RJ, Jang C, Teng X, Lu W, et al. Glucose feeds the TCA cycle via circulating lactate. Nature 2017;551:115–8.
39. Hensley CT, Faubert B, Yuan Q, Lev-Cohain N, Jin E, Kim J, et al. Metabolic heterogeneity in human lung tumors. Cell 2016;164:681–94.
40. Deaglio S, Morra M, Mallone R, Ausiello CM, Prager E, Garbarino G, et al. Human CD38 (ADP-ribosyl cyclase) is a counter-receptor of CD31, an Ig superfamily member. J Immunol 1998;160:395–402.
41. Ferrero E, Malavasi F. Human CD38, a leukocyte receptor and ectoenzyme, is a member of a novel eukaryotic gene family of nicotinamide adenine dinucleotide+-converting enzymes: extensive structural homology with the genes for murine bone marrow stromal cell antigen 1 and aplysian ADP-ribosyl cyclase. J Immunol 1997;159:3858–65.
42. Liu X, Grogan TR, Hieronymus H, Hashimoto T, Mottahedeh J, Cheng D, et al. Low CD38 identifies progenitor-like inflammation-associated luminal cells that can initiate human prostate cancer and predict poor outcome. Cell Rep 2016;17:2596–606.
43. Fernandez JE, Deaglio S, Donati D, Beusan IS, Corno F, Aranega A, et al. Analysis of the distribution of human CD38 and of its ligand CD31 in normal tissues. J Biol Regul Homeost Agents 1998;12:81–91.
44. Morandi F, Morandi B, Horenstein AL, Chillemi A, Quarona V, Zaccarello G, et al. A non-canonical adenosinergic pathway led by CD38 in human melanoma cells induces suppression of T cell proliferation. Oncotarget 2015;6:25602–18.
45. Lee CU, Song EK, Yoo CH, Kwak YK, Han MK. Lipopolysaccharide induces CD38 expression and solubilization in J774 macrophage cells. Mol Cells 2012;34:573–6.
46. Pepping JK, Vandanmagsar B, Fernandez-Kim SO, Zhang J, Mynatt RL, Bruce-Keller AJ. Myeloid-specific deletion of NOX2 prevents the metabolic and neurologic consequences of high fat diet. PLoS One 2017;12: e0181500.
47. Quarona V, Zaccarello G, Chillemi A, Brunetti E, Singh VK, Ferrero E, et al. CD38 and CD157: a long journey from activation markers to multifunctional molecules. Cytometry B Clin Cytom 2013;84:207–17.
48. Christen S, Lorendeau D, Schmieder R, Broekaert D, Metzger K, Veys K, et al. Breast cancer-derived lung metastases show increased pyruvate carboxylase-dependent anaplerosis. Cell Rep 2016;17:837–48.